J Mol Model (2013) 19:5501–5513
DOI 10.1007/s00894-013-2054-y

ORIGINAL PAPER

A density functional theory study on peptide bond cleavage at aspartic residues: direct vs cyclic intermediate hydrolysis

Wichien Sang-aroon · Vittaya Amornkitbamrung · Vithaya Ruangpornvisuti

Received: 10 July 2013 / Accepted: 28 October 2013 / Published online: 17 November 2013

Abstract In this work, peptide bond cleavages at carboxy- and amino-sides of the aspartic residue in a peptide model via direct (concerted and step-wise) and cyclic intermediate hydrolysis reaction pathways were explored computationally. The energetics, thermodynamic properties, rate constants, and equilibrium constants of all hydrolysis reactions, as well as their energy profiles were computed at the B3LYP/6-311++G(d,p) level of theory. The result indicated that peptide bond cleavage of the Asp residue occurred most preferentially via the cyclic intermediate hydrolysis pathway. In all reaction pathways, cleavage of the peptide bond at the amino-side occurred less preferentially than at the carboxy-side. The overall reaction rate constants of peptide bond cleavage of the Asp residue at the carboxy-side for the assisted system were, in increasing order: concerted < step-wise < cyclic intermediate.

Keywords Aspartic residue · Peptide bond cleavage · Hydrolysis · DFT · Hydrolytic catalyst

W. Sang-aroon (✉)
Department of Chemistry, Faculty of Engineering, Rajamangala University of Technology Isan, Khonkaen Campus, Srichan Road, Naimuang, Muang District, Khonkaen 40000, Thailand
e-mail: wichien.sa@rmuti.ac.th

V. Amornkitbamrung
Integrated Nanotechnology Research Center, Department of Physics, Faculty of Science, Khon Kaen University, Khonkaen 40002, Thailand

V. Ruangpornvisuti
Supramolecular Chemistry Research Unit, Department of Chemistry, Faculty of Science, Chulalongkorn University, Phyathai Road, Pathumwan, Bangkok 10320, Thailand

Introduction

Hydrolysis of peptide bonds in a peptide/protein backbone is the major route of protein degradation as well as in protein oxidation [1, 2], deamidation [3, 4] and other mechanisms [5]. A number of theoretical [6–8] and experimental [9–12] studies have focused on the hydrolysis of peptide bonds in peptides/proteins because of its important biological relevance. A number of peptide bond hydrolytic pathways at neutral pH have been proposed by Gorb et al. [13]. Plausible hydrolysis pathways involving water-catalytic reactions are shown in Scheme 1. Cascella et al. [14] concluded that hydrolysis of formamide in neutral pH involves a zwitterionic intermediate ZW1 following nucleophilic attack by water on the carbonyl carbon. A hydrolytic reaction via ZW2 by two or more water molecules attacking the carbonyl carbon and amino nitrogen was reported by Zhan et al. [15]. The reaction pathway proceeds via an amino-gem-diol intermediate with two or more water molecules attacking the carbonyl carbon accompanied by proton transfer from the water to the carbonyl oxygen, i.e., a concerted reaction pathway [13]. Recently, ab initio molecular dynamic studies have shown that no zwitterionic intermediate (ZW2) is found, and that the concerted reaction results in peptide bond cleavage [16]. A similar work studied the acid-catalyzed hydrolysis of peptide bonds in model compounds via an amino-gem-diol intermediate pathway [17]. An acid-assisted hydrolysis of formamide with O- and N-prototonated pathways has also been studied by means of quantum mechanical methods [18].

As mentioned above, hydrolysis can occur due not only to direct nucleophilic attack of water on the carbonyl carbon of the peptide bond but also to other factors. In the case of Asn residues, hydrolysis of a cyclic imide intermediate (formed from nucleophilic attack of the side-chain amide nitrogen on the backbone carbonyl carbon) leads to cleavage of the peptide bond [19, 20]. Similarly, degradation of Asp residues has

Scheme 1 Plausible pathways of peptide bond cleavage due to hydrolytic reactions [14]

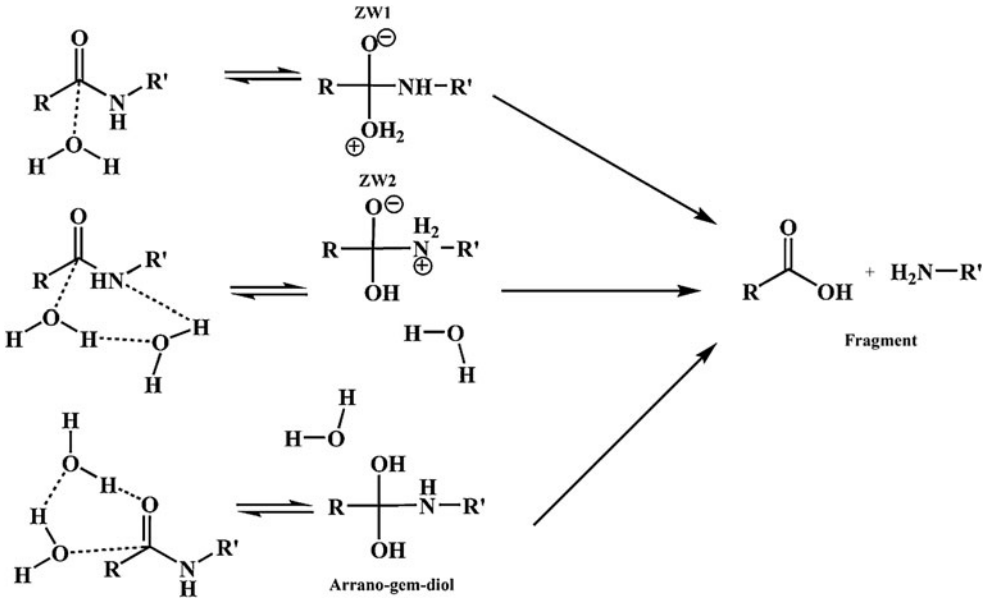

been evidenced to occur via hydrolysis of the cyclic anhydride forming from nucleophilic attack by a side-chain carboxyl on the backbone carbonyl. Peptide bond cleavage at Asp and Glu residues has been reported in peptides and proteins [21–24]. Degradation of peptide bonds in aqueous solution at the Asp residue in a hexapeptide (Val-Tyr-Pro-Asp-Gly-Ala) model has been proved experimentally. It was found that degradation is a function of pH, buffer concentration and temperature [25]. The solvent isotropic method has been studied to distinguish the rate and mechanism of peptide bond cleavage between direct hydrolysis and cyclic anhydride hydrolysis. The results showed that it is difficult to determine the main degradation pathway based on these reactions.

Thus, to distinguish the two reaction pathways, this work reports the energies, reaction rates, equilibrium constants as well as thermodynamic quantities for the peptide bond cleavage mechanism at an Asp residue in a peptide model using density functional theory (DFT) calculation methods. The reaction mechanisms via concerted, step-wise direct hydrolysis and cyclic intermediate pathways were studied. Peptide bond cleavages at both the carboxy- and amino-sides were examined. The calculations were performed in neutral form even though the Asp residue presents as an anionic species due to the fact that the β-hydroxyl proton must be involved to complete the reaction. The results are discussed independently of pH conditions and other factors that can affect to the rate and mechanism.

Computational methods

The Asp residue in the model peptide used in this calculation work is shown in Fig. 1. The geometries of reactants, transition states, intermediates and products were fully optimized in gas phase using DFT [26–29] at B3LYP/6-311++G(d,p) level [30–32]. Zero-point energy (ZPE) corrections and thermodynamic properties of all relevant structures were obtained by vibrational frequency calculation at 1 atm and 298.15 K; the frequency was not scaled. Local minima and first-order saddle points were identified by the number of imaginary vibrational frequencies. Solvent effects were taken into account by utilizing the polarize continuum model (PCM) with the integral equation formalism-polarizable continuum (IEF-PCM) model [33–37]. Solvation free energy (ΔG_{sol}) were obtained by single-point calculation of the gas phase-B3LYP/6-311++G(d,p) geometrical structure at the same level in H_2O medium (ε=78.37). The cavity model used for solvent effect calculation was the united atom topological model for Khon-Sham (UAKS) [38, 39]. All calculations were performed with the Gaussian 03 program [40]. The molecular graphics of all related species were generated with the MOLEKEL 4.3 program [41].

The standard enthalpy (ΔH^{o}_{298}) and Gibbs free energy changes (ΔG^{o}_{298}) for all reactions were derived from frequency calculations at the B3LYP/6-311++G(d,p) level of theory. The rate constant k(T), based on transition state theory, was computed from the Gibbs free energy of activation, $\Delta^{\dagger}G^{o}$

Fig. 1 Asp residue modeled peptide used in this work

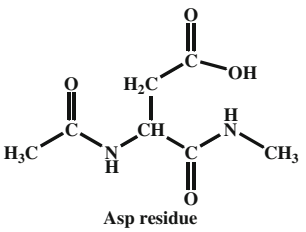

using Eq. (1) [42, 43] and the activation energy, $\Delta^{\dagger}E^{o}$ using Eq. (2) [44].

$$k(T) = \frac{k_B t}{hc^{o}} \exp\left(-\Delta^{\dagger}G^{o}/RT\right) \quad (1)$$

$$k(T) = \kappa \frac{k_B T}{h} \frac{Q_{TS}}{Q_{REA}} \exp\left(-\Delta^{\dagger}E^{o}/RT\right) = \kappa A \exp\left(-\Delta^{\dagger}E^{o}/RT\right) \quad (2)$$

where c° is the concentration factor, k_B is the Boltzmann's constant, h is Plank's constant, T is the absolute temperature, and R is the gas constant. Q_{TS} and Q_{REA} are the partition functions of the transition state and reactant of the reaction, whose values are composed of translational, rotational, and vibrational partition functions. The tunneling coefficient (κ) can be computed with the Wigner method [43, 45–47] as $\kappa = \frac{1}{24}\left(\frac{h\nu_i}{k_B T}\right)^2$ where ν_i is the imaginary frequency that accounts for the vibration motion along the reaction path. The pre-exponential factor (A) is defined as $A = \frac{k_B T}{h}\frac{Q_{TS}}{Q_{REA}}$. The equilibrium constant K at standard temperature and pressure was computed using a thermodynamic equation $K = \exp(-\Delta G^{\circ}/RT)$.

Results and discussion

Concerted hydrolysis

The reaction mechanisms of unassisted- and assisted concerted hydrolysis at the carboxy- and amino-sides are shown in Scheme 2. Peptide bond cleavage is due to nucleophilic attack by water molecules on the backbone carbonyl. The hydrolytic proton is transferred and protonated on the amino nitrogen, leading to cleavage of the peptide bond. Relative free energy profiles for concerted hydrolysis of unassisted- and assisted reactions at carboxy- and amino-sides are shown in Figs. 2 and 3. Reaction energies, thermodynamic quantities, equilibrium and rate constants of concerted hydrolysis at carboxy- and amino-sides computed at the B3LYP/6-311++G(d,p) level of theory are tabulated in Tables 1 and 2, respectively. Values of 46.7(45.2) and 39.86(42.89) kcal mol^{-1} activation free barriers were required for unassisted- and assisted systems for cleavage at the carboxy-side, respectively. Activation free barriers of 52.3(50.6) and 43.8(45.0) kcal mol^{-1} were required for unassisted- and assisted systems for cleavage at the amino-side, respectively. As a result, cleavage at the carboxy-side is thermodynamically preferred to cleavage at the amino-side. A catalytic effect due to the explicit water molecule plays an important role in lowering the energy barrier of the reaction. Rate constants for the reactions computed based on Eq. 1 (Table 1) and Eq. 2 (Table 2) did not differ much. Equilibrium constants for cleavage at the amino-side were higher than those for cleavage at the carboxy-side, especially in the assisted system. It was noted that peptide bond cleavage at the amino-side was preferred thermodynamically while cleavage at the carboxy-side was kinetically and energetically favorable.

Here, we performed calculations on unassisted systems of cleavage at the carboxy-side to see how the B3LYP performs in terms of reaction barriers. The dispersion-corrected functional M06-2X [48] was used for calculation to allow comparison with B3LYP calculations. This is due to the similarity of the model and some reaction pathways studied in this work and our previous work [49]. The unassisted reaction at the carboxy-side is shown to compare the energies, thermodynamics, rate and equilibrium constants between M06-2X and B3LYP calculations (see Tables 1, 2). M06-2X calculation results showed that activation energy and free energy barrier values were approximately 2 and 3 kcal mol^{-1} lower than those of B3LYP calculations. Similarly, reaction enthalpy and free energy of the M06-2X functional differs from M06-2X to B3LYP by 2–3 kcal mol^{-1}. Rate constants computed based on Eqs. 1 and 2, as well as the equilibrium constant for the M06-2X functional were 1.78×10^{-19} and 4.04×10^{-19} and 6.99×10^{-5}, respectively; this under- and over-estimates the values found in B3LYP compare to those of M06-2X by a factor of 10^{-3} and 10^{-2}, respectively. However, it has been reported that B3LYP activation barriers overestimate experimental values by 3–4 kcal mol^{-1} while M06-2X activation barrier underestimate the experimental value by 2.8–3.7 kcal mol^{-1} [50]. Thus, the activation barrier as well as rate constants based on the B3LYP functional calculation used in this work are acceptable.

As can be seen in Fig. 2, a hydrogen bond between the backbone amino hydrogen and the side-chain carboxyl oxygen is also present in the reactant and transition state (TS1C_w and TS1C _w2) structures of both systems. In contrast, hydrogen bonding is not found in the reactants but is found in the transition state (TS1N_w and TS1N _w2) structures for cleavage at amino-side reactions (Fig. 3). The change in side-chain conformation at the TS of the reactants may be due to steric hindrance and also affects the energy barrier of the reaction. Based on the optimized structure of the TS, the breaking C–N bond of TS1_w2 is shorter than those of TS1_w2 at both carboxy- and amino-sides. Similarly, the distance between the hydrolytic proton and the backbone amino nitrogen is also shorter due to the assistance of one additional water molecule.

Step-wise hydrolysis (amino-gem-diol intermediate)

The reaction mechanisms of unassisted- and assisted step-wise hydrolysis at carboxy- and amino-sides are shown in Scheme 3. Peptide bond cleavage for step-wise hydrolysis requires two reaction steps. The first step occurs via

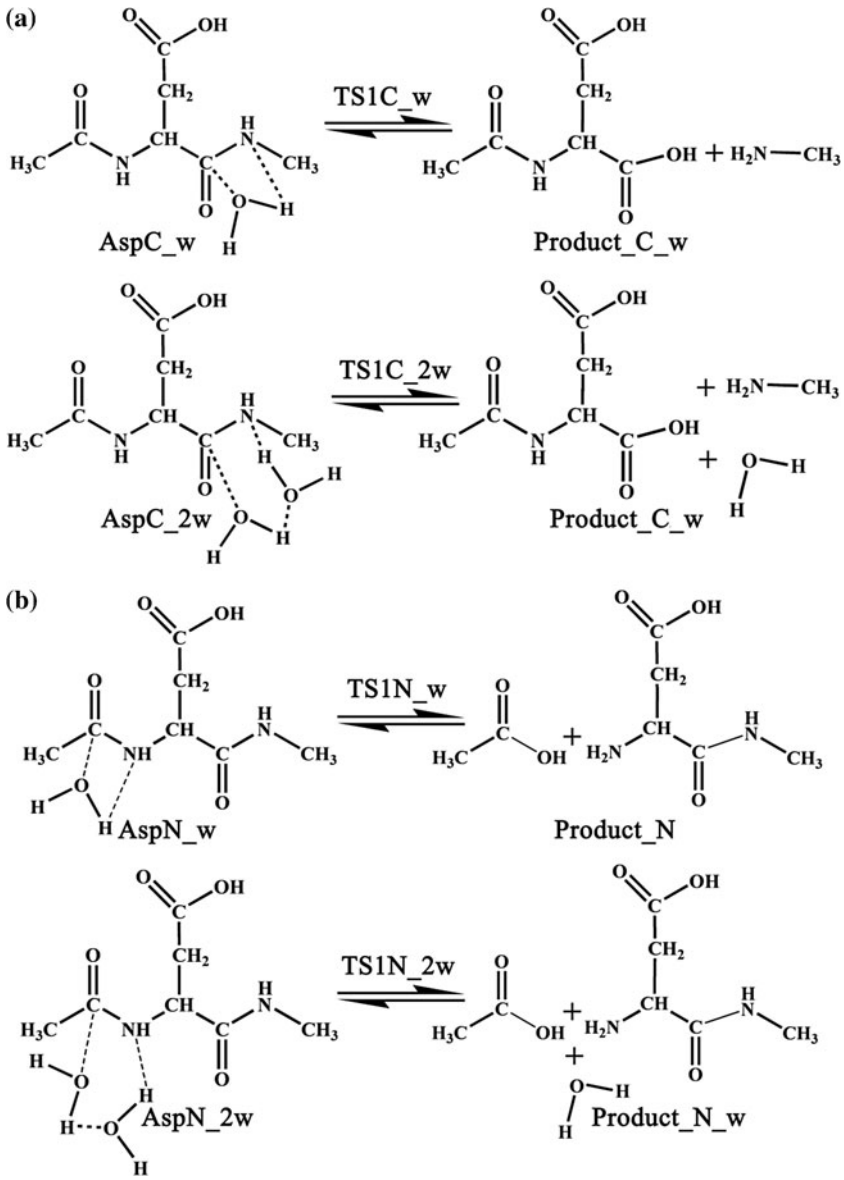

Scheme 2 Peptide bond cleavage mechanism of Asp residue via concerted hydrolysis at (**a**) carboxy-side and (**b**) amino-side

nucleophilic attack by a water molecule on the backbone carbonyl. The hydrolytic proton is transferred and protonated on the carbonyl oxygen, forming an amino-gem-diol intermediate (TS2Ca_w/w2). The second step involves breaking of the C–N bond due to proton transfer from the protonated carbonyl oxygen to the amino nitrogen. Relative free energy profiles for concerted hydrolysis of unassisted- and assisted reactions at carboxy- and amino-sides are shown in Figs. 4 and 5. Energies of reactions, thermodynamic quantities, equilibrium and rate constants of step-wise hydrolysis at carboxy- and amino-sides computed at the B3LYP/6-311++G(d,p) level of theory are reported in Tables 3 and 4, respectively.

For cleavage at the carboxy-side, the first reaction step (Asp→TS2Ca_w/w2→INT2C_w/w2) requires an activation free energy barrier of 47.5(50.5) and 40.3(43.5) kcal mol^{-1} for unassisted- and assisted systems, respectively, while 25.8(27.3) and 8.7(6.7) kcal mol^{-1} are required for the second reaction step (INT2C_w/w2→TS2Cb_w/w2→Cleavage product1/2) of unassisted- and assisted systems. The corresponding rate constants for each step are 9.1×10^{-23}, 7.5×10^{-7} and 1.7×10^{-17}, 2.5×10^{-6} s^{-1} for unassisted- and assisted systems. Rate constants computed based on tunneling effects (tabulated in Table 4) are in agreement with those of activation free energies in Table 3. Based on the barriers of each reaction step, it was noted that the first step is the rate determining step (RDS). The second step has the highest barrier to the overall reaction (50.8 and 38.0 kcal mol^{-1}). Thus, the rate constant for the overall reaction is computed based on the barrier of TS2Cb_w and TS2Cb_w2 for unassisted and assisted systems, respectively (discussed further below).

Figure 5 represents the relative free energy profile of unassisted- and assisted systems for step-wise direct hydrolysis

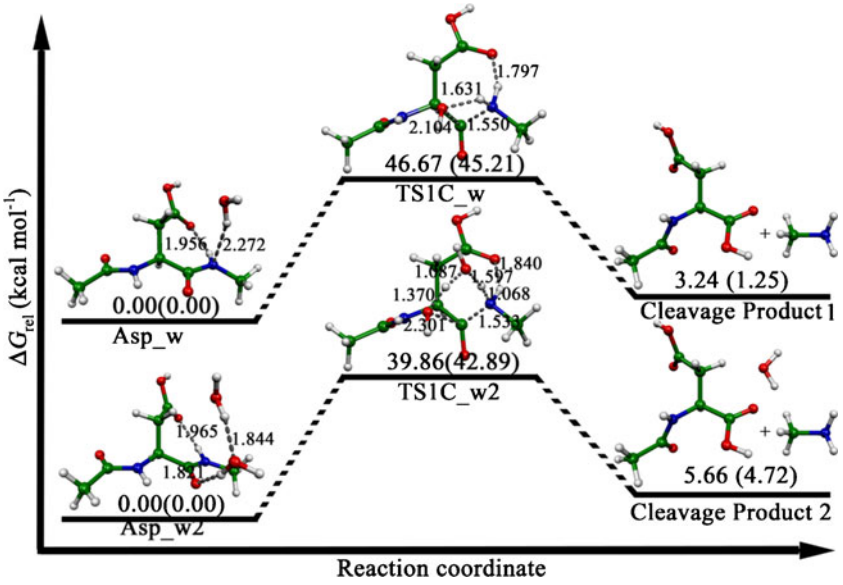

Fig. 2 Relative free energy profile for concerted unassisted- and assisted peptide bond cleavage at the carboxy-side. Relative free energies computed in continuum media are in *parenthesis*. Bond lengths are in Angstrom

at the amino-side. The cleavage proceeds via two reactions: Asp→TS2Na_w/w2→INT2N_w/w2 and INT2N_w/w2→TS2Nb_w/w2→Cleavage product 3/4. Activation free energies required for the first and second steps of the unassisted system are 52.8 and 29.1, and for the assisted system are 41.4, 20.1 kcal mol^{-1}, respectively. The corresponding rate constants are 1.3×10^{-26}, 3.2×10^{-9} and 2.9×10^{-18}, 1.2×10^{-2} s^{-1} for unassisted- and assisted-systems. Based on the barriers of each reaction step, it was also noted that the first step is the RDS while the second step has the highest barrier for the overall reaction (56.4 and 43.1 kcal mol^{-1}). Thus, the rate constant for the overall reaction is computed based on the barrier of TS2Nb_w and TS2Nb_w2 for unassisted and assisted systems, respectively (discussed further below).

It can be stated that the step-wise reactions for peptide bond cleavage at both carboxy- and amino-sides occur less preferentially than those of the concerted pathways based on both RDS and the highest barrier to the reactions. The computational result is in agreement with previous work in which direct hydrolysis of peptide bond via the ZW pathway was not found but resulted from concerted hydrolysis [16].

Cyclic intermediate hydrolysis

Peptide bond cleavage at carboxy- and amino-sides via cyclic intermediate formation is shown in Scheme 3. This reaction pathway has been studied and reported previously [49]. The present work does not presented the fates of intermediate hydrolysis as this has been done previously. For the peptide bond at the carboxy-side, there are two steps of hydrolysis including cyclic anhydride intermediate formation (Asp→TS3Ca_w/w2→INT3C_w/w2) followed by its hydrolysis

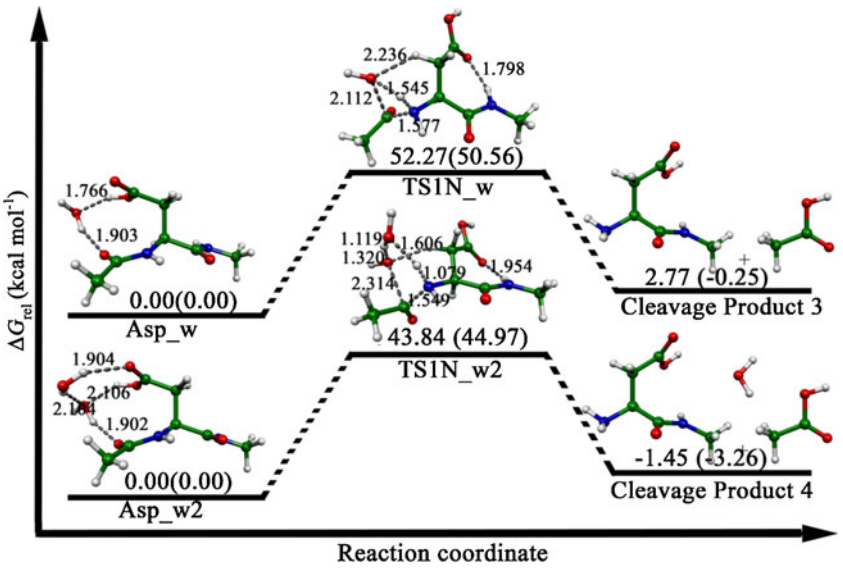

Fig. 3 Relative free energy profiles for concerted unassisted- and assisted peptide bond cleavages at the amino-side. Relative free energies computed in continuum media are in *parenthesis*. Bond lengths are in Angstrom

Table 1 Energies, thermodynamic properties, rate constants and equilibrium constants of concerted hydrolysis reaction for unassisted- and assisted systems

Reaction	$\Delta^{\dagger}E$ (kcal/mol)	$\Delta^{\dagger}G$ (kcal/mol)	k_{298} (s^{-1})	ΔE (kcal/mol)	ΔG_{298} (kcal/mol)	ΔH_{298} (kcal/mol)	K_{298}
Carboxy-side							
Unassisted							
Asp_w→TS1C_w→product[a]	44.26 (42.52)[a]	46.67 (43.01)	3.79×10^{-22} (1.78×10^{-19})	14.14 (14.77)	3.24 (5.67)	13.59 (16.06)	4.19×10^{-3} (6.99×10^{-5})
Assisted							
Asp_2w→TS1C_2w→product	38.20	39.86	3.71×10^{-17}	25.12	5.66	25.32	7.07×10^{-5}
Amino-side							
Unassisted							
Asp_w→TS1N_w→product	50.62	52.24	3.14×10^{-26}	15.19	2.77	14.95	9.34×10^{-3}
Assisted							
Asp_2w→*TS*1N_2w→product	41.95	43.84	4.53×10^{-20}	20.39	−1.45	20.82	1.15×10^{1}

[a] Values in parenthesis are at the M06-2X/6-311++G(d,p) level

(INT3C_w/w2→TS3Cb_w/w2→Cleavage product5/6) leading to peptide bond degradation. The relative free energy profile for unassisted- and assisted systems at the carboxy-side is shown in Fig. 6. Corresponding reaction energies, thermodynamic quantities, equilibrium and rate constants are given in Table 5. Relative free energies for the first and second steps are 20.9(18.5), 34.4(31.8) and 15.3(14.5), 29.9(31.7) kcal mol^{-1}, respectively, for unassisted- and assisted systems. Either the first or second step can be assigned as the RDS as their barriers are proximal. Cleavage at the carboxy-side of the Asp residue is more energetically and kinetically favorable than cleavage via the direct concerted and step-wise pathways. This result is in agreement with previous experimental and theoretical studies that concluded that peptide bond cleavage at Asp residues occurs via hydrolysis of a cyclic anhydride intermediate in the context of direct hydrolysis [19, 49, 50].

For cleavage at the amino-side, peptide bond cleavage comprises three reaction steps, including (1) formation of six-membered ring intermediate, (2) hydrolysis of the cyclic intermediate, and (3) cleavage of the peptide bond as shown in Scheme 4. Relative free energy profiles for unassisted- and assisted systems for cleavage at the amino-side are shown in Fig. 7. The corresponding reaction energies, thermodynamic quantities, equilibrium and rate constants are tabulated in Tables 5 and 6. The activation free barrier for the three reaction steps of the unassisted system are 25.3, 14.7 and 34.0 kcal mol^{-1}, and for assisted systems are 19.4, 6.7 and 40.4 kcal mol^{-1}, respectively. Rate constants of these three steps for the unassisted system are 1.7×10^{-6}, 1.1×10^{-6} and 7.7×10^{-13} s^{-1} and for the assisted system are 3.68×10^{-2}, 7.5×10^{-7} and 1.6×10^{-17} s^{-1}, respectively. The RDS is assigned to the third reaction step (INT3Nb_w/w2→TS3Nc_w/w2→

Table 2 Activation energies, tunneling coefficients, A factors and rate constants of concerted hydrolysis reaction for unassisted- and assisted systems

Reaction	κ[a]	Q_{TS}/Q_{REA}	A[b]	$\Delta^{\dagger}E$ (kcal/mol)	k_{298} (s^{-1})
Carboxy-side					
Unassisted					
Asp_w→TS1C_w→product[c]	1.12 (1.02)[c]	1.57×10^{-2} (7.97×10^{-2})	9.77×10^{10} (4.41×10^{11})	44.26 (42.52)	3.93×10^{-22} (4.04×10^{-19})
Assisted					
Asp_2w→TS1C_2w→product	1.05	2.13×10^{-3}	1.32×10^{10}	38.20	1.38×10^{-18}
Amino-side					
Unassisted					
Asp_w→TS1N_w→product	1.17	6.08×10^{-2}	3.96×10^{11}	50.62	3.62×10^{-26}
Assisted					
Asp_2w→TS1N_2w→product	1.15	4.02×10^{-2}	2.50×10^{1}	41.95	5.06×10^{-20}

[a] $\kappa = 1 + \frac{1}{24}\left(\frac{h\nu_i}{k_B T}\right)^2$

[b] $A = \frac{k_B T}{h}\frac{Q_{TS}}{Q_{REA}}$, in s^{-1}

[c] Values in parenthesis are at the M06-2X/6-311++G(d,p) level

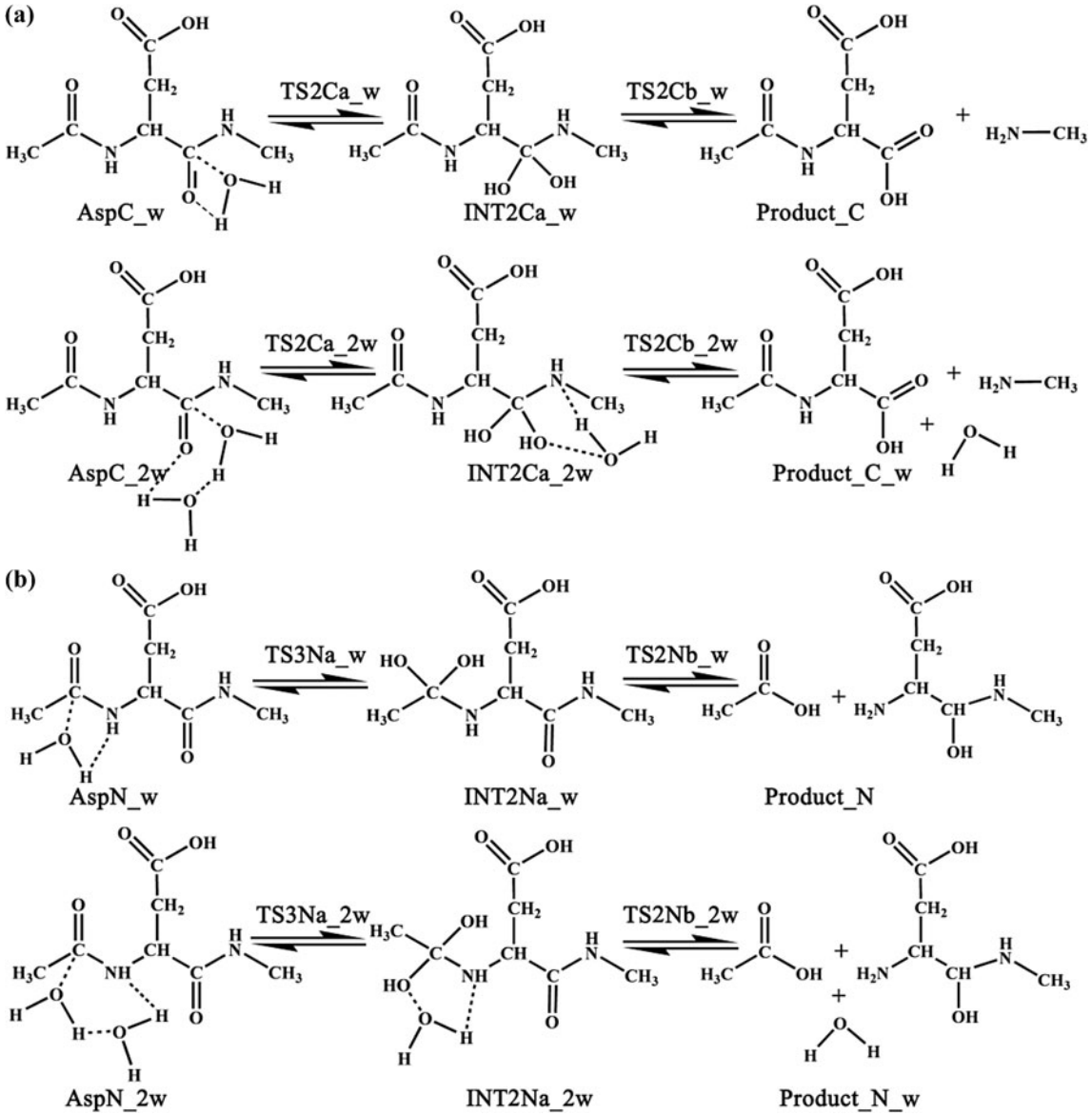

Scheme 3 Peptide bond cleavage mechanism of Asp residue via step-wise hydrolysis at (**a**) carboxy-side and (**b**) amino-side

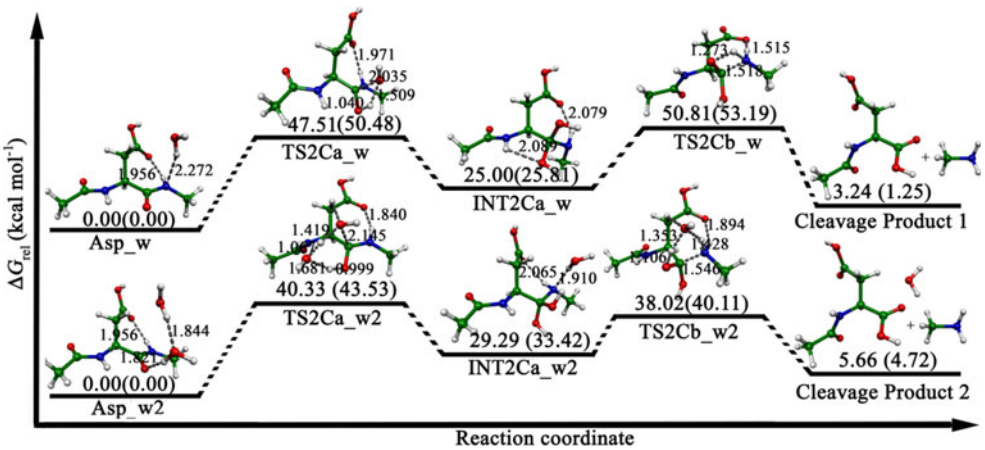

Fig. 4 Relative free energy profiles for stepwise unassisted- and assisted peptide bond cleavage at carboxy-side. Relative free energies computed in continuum media are in *parenthesis*. Bond lengths are in Angstrom

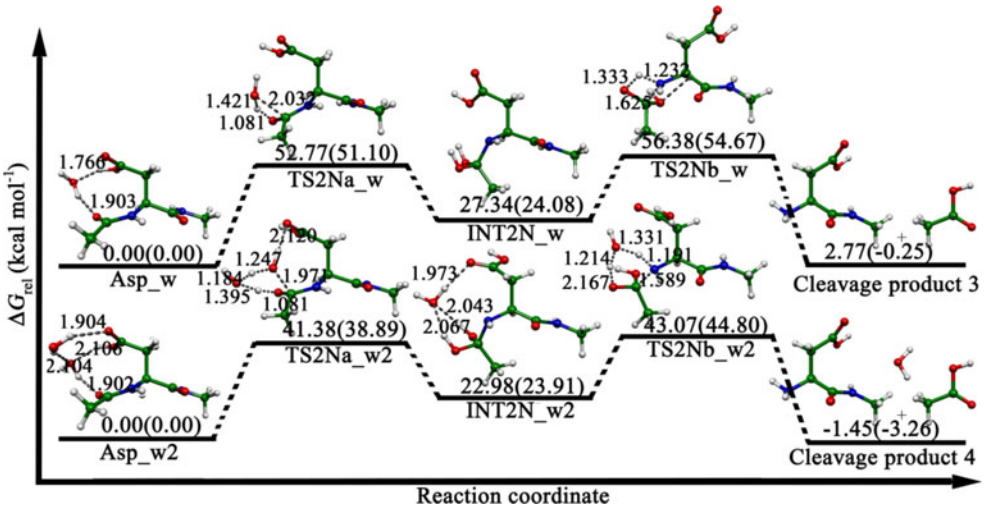

Fig. 5 Relative free energy profiles for step-wise unassisted- and assisted peptide bond cleavage at amino-side. Relative free energies computed in continuum media are in *parenthesis*. Bond lengths are in Angstrom

cleavage product). This reaction step requires a relative barrier of up to 55 and 60 kcal mol^{-1} for both systems. This may be due to the conformational strength of the transition states. This highest barrier is then used to compute the overall reaction rate constant.

The results show that cleavage at the amino-side of the Asp residue is less kinetically and energetically favorable than that at the carboxy-side, despite the fact that the six-membered ring (INT3Na_w/w2) is expected to be more thermodynamically stable than the five-membered ring (INT3C_w/w3) [51]. Based on previous experimental results, it was concluded that pyrolysis of protein at the temperature range between 220 °C and 250 °C is undergone favorably cleavage at the C-terminus via the cyclic anhydride intermediate rather than cleavage at the N-terminus [50]. Model studies on peptides have shown that cyclic imide formation in peptides can also lead to peptide bond cleavage [52]. Spontaneous peptide bond cleavage in aging alpha-crystallin through a succinimide intermediate has been reported [53, 54]. It is expected that cleavage of both asparagine and aspartic acid amide occurred at the C-terminal end of the truncated polypeptide, as in the case of the alpha A-(1-101)-chain—the first example of non-enzymatic in vivo peptide bond cleavage in an aging protein through the formation of a succinimide intermediate.

The overall reaction energies, thermodynamic properties, rate and equilibrium constants of peptide bond cleavage of the three reaction pathways for unassisted- and assisted systems are summarized in Table 7. The overall rate constant is computed based on the highest activation barrier for each overall reaction pathway. Overall reaction rate constants for cleavage at the carboxy-side for unassisted- and assisted systems are, in deceasing order: cyclic intermediate (3.85×10^{-13} s^{-1}) >

Table 3 Energies, thermodynamic properties, rate constants and equilibrium constants of step-wise hydrolysis reaction for unassisted- and assisted systems

Reaction	$\Delta^{\dagger}E$ (kcal/mol)	$\Delta^{\dagger}G$ (kcal/mol)	k_{298} (s^{-1})	ΔE (kcal/mol)	ΔG_{298} (kcal/mol)	ΔH_{298} (kcal/mol)	K_{298}
Carboxy-side							
Unassisted							
Asp_w→TS2Ca_w→INT2Ca_w	45.07	47.51	9.15×10^{-23}	22.36	25.00	20.87	4.71×10^{-19}
INT2Ca_w→TS2Cb_w→product	25.48	25.81	7.51×10^{-7}	−8.21	−21.76	−7.28	8.88×10^{15}
Assisted							
Asp_2w→TS2Ca_2w→INT2Ca_2w	36.83	40.33	1.69×10^{-17}	25.69	29.29	24.24	3.39×10^{-22}
INT2Ca_2w→TS2Cb_2w→product	7.90	8.73	2.47×10^{-6}	−8.47	−32.36	−5.86	5.24×10^{23}
Amino-side							
Unassisted							
Asp_w→TS2Na_w→INT2Na_w	51.83	52.77	1.28×10^{-26}	26.20	27.34	25.35	9.13×10^{-21}
INT2Na_w→TS2Nb_w→product	29.36	29.05	3.16×10^{-9}	−11.01	−24.57	−10.40	1.02×10^{18}
Assisted							
Asp_2w→TS2Na_2w→INT2Na_2w	39.94	41.38	2.90×10^{-18}	23.23	22.98	22.39	1.42×10^{-17}
INT2Na_2w→TS2Nb_2w→product	18.06	20.09	1.17×10^{-2}	−2.85	−24.43	−1.58	8.05×10^{17}

Table 4 Activation energies, tunneling coefficients, A factors and rate constants of step-wise hydrolysis reaction for unassisted- and assisted systems

Reaction	κ[a]	Q_{TS}/Q_{REA}	A[b]	$\Delta^{\dagger}E$ (kcal/mol)	k_{298} (s^{-1})
Carboxy-side					
Unassisted					
Asp_w→TS2Ca_w→INT2Ca_w	1.37	1.47×10^{-2}	9.16×10^{10}	45.07	1.14×10^{-22}
INT2Ca_w→TS2Cb_w→product	3.73	5.98×10^{-1}	3.71×10^{12}	25.48	2.92×10^{-6}
Assisted					
Asp_2w→TS2Ca_2w→INT2Ca_2w	1.06	2.26×10^{-3}	1.41×10^{10}	36.83	1.50×10^{-17}
INT2Ca_2w→TS2Cb_2w→product	1.08	2.24×10^{-1}	1.39×10^{12}	7.90	2.45×10^{6}
Amino-side					
Unassisted					
Asp_w→TS2Na_w→INT2Na_w	1.98	1.94×10^{-1}	1.20×10^{12}	51.83	2.41×10^{-26}
INT2Na_w→TS2Nb_w→product	3.66	1.73×10^{0}	1.08×10^{13}	29.36	1.18×10^{-8}
Assisted					
Asp_2w→TS2Na_2w→INT2Na_2w	2.10	8.53×10^{-2}	5.30×10^{11}	39.94	5.86×10^{-18}
INT2Na_2w→TS2Nb_2w→product	2.72	3.13×10^{-2}	1.95×10^{11}	18.06	3.03×10^{-2}

[a] $\kappa = 1 + \frac{1}{24}\left(\frac{h\nu_i}{k_B T}\right)^2$

[b] $A = \frac{k_B T}{h}\frac{Q_{TS}}{Q_{REA}}$, in s^{-1}

concerted (3.67×10^{-22} s^{-1}) > stepwise (3.37×10^{-25} s^{-1}) and cyclic intermediate (7.82×10^{-10} s^{-1}) > stepwise (8.10×10^{-16} s^{-1}) > concerted (3.62×10^{-17} s^{-1}). Surprisingly, the overall reaction rate constants for cleavage at the amino-side for unassisted systems are, in deceasing order: concerted (3.02×10^{-26} s^{-1}) > cyclic intermediate (7.77×10^{-29} s^{-1}) ~ stepwise (2.77×10^{-29} s^{-1}); and for assisted system: stepwise (1.60×10^{-20} s^{-1}) > concerted (4.37×10^{-20} s^{-1}) > cyclic intermediate (1.00×10^{-31} s^{-1}). Based on the overall reaction rate constant, it can be said that peptide bond cleavage at an Asp residue via cyclic intermediate formation at the carboxy-side is the most favorable pathway. Conversely, the most favored pathways for peptide bond cleavage at the amino-side are the concerted and step-wise hydrolysis reaction pathway for unassisted and assisted systems, respectively. In addition, the overall equilibrium constant found upon cleavage at the amino-side is higher than that at the carboxy-side, especially in the cyclic intermediate reaction pathway. This confirms here that peptide bond cleavage at the amino-side is thermodynamically stable but not kinetically and energetically stable as discussed above. However, it can be concluded that cleavage at the amino-side is inhibited by cleavage at the carboxy-side via the cyclic intermediate formation pathway.

Conclusion

The energetics, thermodynamic properties, rate constants, and equilibrium constants of three peptide bond hydrolysis

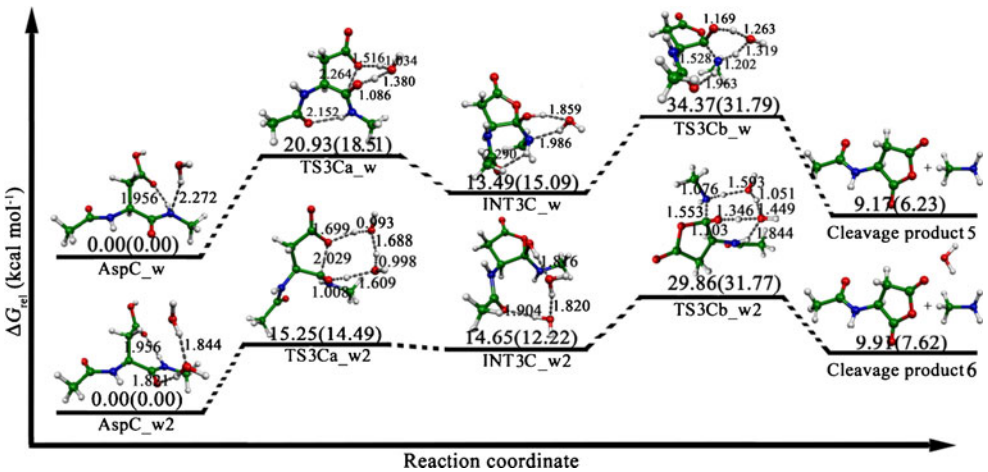

Fig. 6 Relative free energy profiles for unassisted- and assisted peptide bond cleavage at the carboxy-side via the cyclic intermediate reaction pathway. Relative free energies computed in continuum media are in *parenthesis*. Bond lengths are in Angstrom. (Optimized-structures of some species in the unassisted pathway are adapted from [48], computed based on the same level of theory)

Table 5 Energies, thermodynamic properties, rate constants and equilibrium constants of peptide bond cleavage via the cyclic intermediate reaction pathway for unassisted- and assisted systems

Reaction	$\Delta^{\dagger}E$ (kcal/mol)	$\Delta^{\dagger}G$ (kcal/mol)	k_{298} (s^{-1})	ΔE (kcal/mol)	ΔG_{298} (kcal/mol)	ΔH_{298} (kcal/mol)	K_{298}
Carboxy-side							
Unassisted							
Asp_w→TS3Ca_w→INT3Ca_w	18.47	20.93	2.78×10^{-3}	13.99	13.49	14.47	2.46×10^{-11}
INT3Ca_w→TS3Cb_w→product	18.86	20.88	3.07×10^{-3}	−0.38	0.65	−10.56	5.57×10^{7}
Assisted							
Asp_2w→TS3Ca_w2→INTCa_w2	14.67	15.25	4.08×10^{1}	13.90	14.65	20.40	1.82×10^{-11}
INT3Ca_w2→TS3Cb_w3→product	14.04	15.21	4.41×10^{1}	7.22	−13.61	9.40	9.56×10^{9}
Amino-side							
Assisted							
Asp_w→TS3Na_w→INT3Na_w	23.69	25.33	1.68×10^{-6}	24.55	24.51	24.29	1.08×10^{-18}
INT3Na_w→TS3Nb_w→INT3Nb_w	13.54	14.69	1.06×10^{2}	−3.95	−2.65	−7.24	2.00×10^{5}
INT3Nb_w→TS3Nc_w→product	31.14	33.97	7.77×10^{-13}	−8.16	−10.25	−10.82	8.70×10^{7}
Assisted							
Asp_w2→TS3Na_w2→INT3Na_w2	18.34	19.41	3.68×10^{-2}	16.76	16.82	17.17	3.68×10^{-2}
INT3Na_w2→TS3Nb_w2→INT3Nb_w2	7.17	6.71	7.50×10^{7}	0.02	−3.73	1.64	5.46×10^{2}
INT3Nb_w2→TS3Nc_w2→product	35.72	40.35	1.64×10^{-17}	−1.98	−20.81	−2.39	2.34×10^{-11}

reactions at the carboxy- and amino-sides for unassisted and assisted systems of the aspartic acid residue in a peptide model were investigated at the DFT/B3LYP/6-311++G(d,p) level of theory. The rate constants of all reactions were obtained based

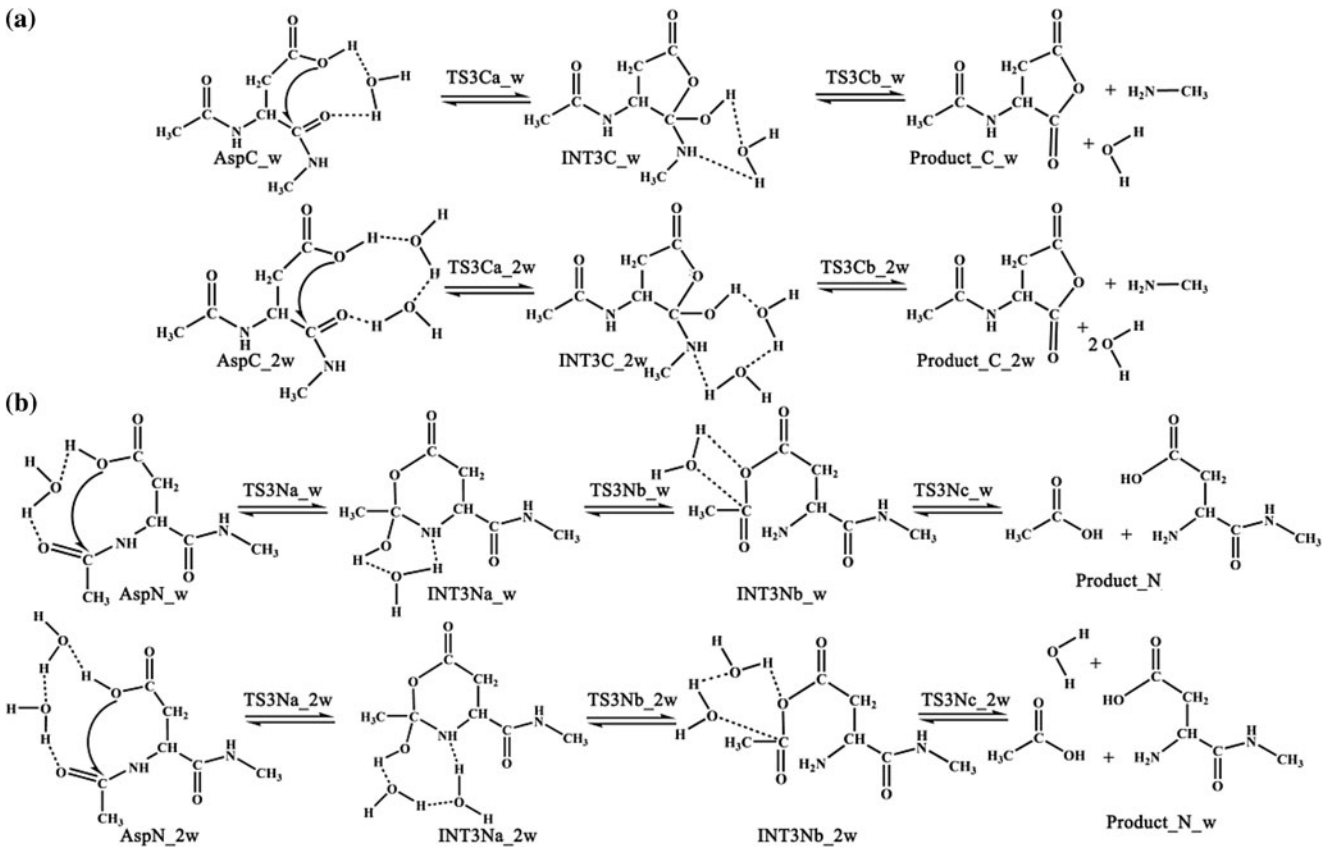

Scheme 4 Peptide bond cleavage mechanism at the Asp residue via cyclic intermediate hydrolysis at (**a**) the carboxy-side and (**b**) amino-side

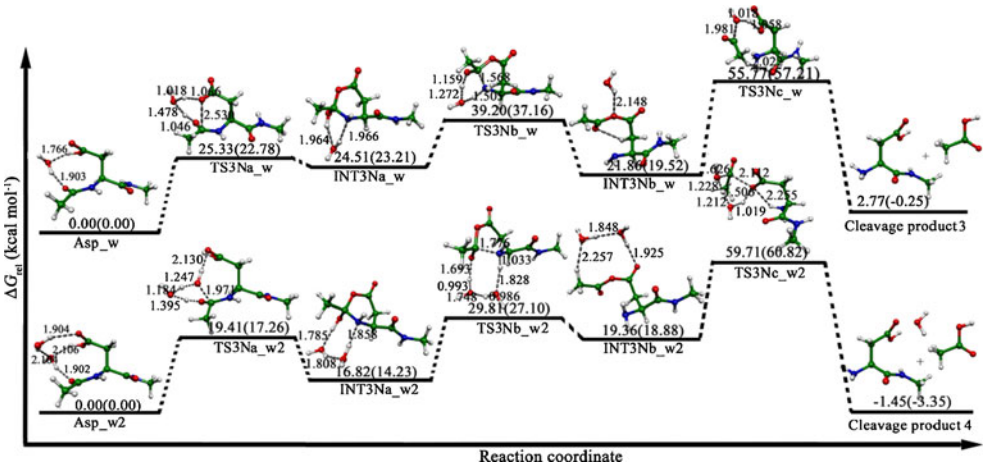

Fig. 7 Relative free energy profiles for unassisted- and assisted peptide bond cleavage at the amino-side via the cyclic intermediate hydrolysis reaction pathway. Relative free energies computed in continuum media are in *parenthesis*. Bond lengths are in Angstrom. (Optimized-structures of some species in unassisted pathway adapted from [48], computed based on the same level of theory)

on the Gibbs free energy of activation (Eq. 1) and on activation energy (Eq. 2).

The results can be summarized as follows:

- Rate constants based on RDS for the three peptide bond cleavages at the carboxy- and amino-sides for both unassisted and assisted systems are, in decreasing order: cyclic intermediate > concerted > step-wise.
- Rate constants based on overall reaction rate constant for cleavage at the carboxy-side in both unassisted- and assisted systems are, in deceasing order: cyclic intermediate > concerted > stepwise. Conversely, overall reaction rate constants for cleavage at the amino-side are, in deceasing order, for unassisted systems: concerted > cyclic intermediate ~ stepwise; and for assisted system: stepwise > concerted > cyclic intermediate.
- Cleavage at the carboxy-side is more favored than cleavage at the amino-side in all reaction pathways.
- The most favored pathway for peptide bond degradation at the Asp residue is cyclic anhydride hydrolysis at the carboxy-side.
- An explicit water molecule plays an important role as a hydrolytic catalyst for peptide bond cleavage.

Table 6 Activation energies, tunneling coefficients, A factors and rate constants of peptide bond cleavage via cyclic intermediate reaction pathway for unassisted- and assisted systems

Reaction	κ[a]	Q_{TS}/Q_{REA}	A[b]	$\Delta^{\dagger}E$ (kcal/mol)	k_{298} (s^{-1})
Carboxy-side					
Unassisted					
Asp_w→TS2Ca_w→INT2Ca_w	1.00	1.86×10^{-1}	1.15×10^{12}	18.47	1.76×10^{-1}
INT2Ca_w→TS2Cb_w→product	1.02	1.87×10^{-1}	1.16×10^{12}	18.86	1.08×10^{-1}
Assisted					
Asp_2w→TS2Ca_2w→INT2Ca_2w	1.00	4.62×10^{-3}	2.87×10^{10}	14.67	5.07×10^{-1}
INT2Ca_2w→TS2Cb_2w→product	1.08	1.38×10^{-1}	8.59×10^{11}	14.04	4.71×10^{1}
Amino-side					
Unassisted					
Asp_w→TS3Na_w→INT3Na_w	1.01	2.72×10^{-1}	1.69×10^{12}	23.69	7.17×10^{-6}
INT3Na_w→TS3Nb_w→INT3Nb_w	1.02	3.27×10^{1}	2.03×10^{14}	13.54	2.39×10^{4}
INT3Nb_w→TS3Nc_w→product	1.00	2.19×10^{-2}	1.36×10^{11}	31.14	1.98×10^{-12}
Assisted					
Asp_w2→TS3Na_w2→INT3Na_w2	1.03	1.64×10^{-1}	1.02×10^{12}	18.34	3.67×10^{-2}
INT3Na_w2→TS3Nb_w2→INT3Nb_w2	1.01	2.24×10^{0}	1.39×10^{13}	7.17	7.74×10^{7}
INT3Nb_w2→TS3Nc_w2→product	1.07	2.93×10^{2}	1.82×10^{15}	35.72	2.34×10^{-11}

[a] $\kappa = 1 + \frac{1}{24}\left(\frac{h\nu_i}{k_B T}\right)^2$

[b] $A = \frac{k_B T}{h}\frac{Q_{TS}}{Q_{REA}}$, in s^{-1}

Table 7 Overall reaction energies, thermodynamic properties, rate and equilibrium constants of peptide bond cleavage of three reaction pathways for unassisted- and assisted systems. Overall rate constant is computed based on the highest barrier in the reactions (see Figs. 2–7)

Reaction	$\Delta^{\dagger}E$ (kcal/mol)	$\Delta^{\dagger}G$ (kcal/mol)	k_{298}[a] (s^{-1})	ΔE (kcal/mol)	ΔG_{298} (kcal/mol)	ΔH_{298} (kcal/mol)	K_{298}
Carboxy-side							
Unassisted systems							
Concerted							
Asp_w→TS1C_w→product	44.26	46.67	3.67×10^{-22}	14.14	3.24	13.59	4.20×10^{-3}
Step-wise							
Asp_w→TS2Cb_w→product	48.82	50.81	3.37×10^{-25}				
Cyclic Intermediate							
Asp_w→TS3Cb_w→product	30.11	34.37	3.85×10^{-13}	20.12	9.17	19.45	1.88×10^{-7}
Assisted systems							
Concerted							
Asp_w2→TS1C_w2→product	38.20	39.86	3.62×10^{-17}	25.12	5.66	25.32	7.06×10^{-5}
Step-wise							
Asp_w2→TS2Cb_w2→product	36.61	38.02	8.10×10^{-16}				
Cyclic Intermediate							
Asp_w2→TS3Cb_w2→product	28.08	29.86	7.82×10^{-10}	21.56	9.91	24.42	5.39×10^{-8}
Amino-side							
Unassisted systems							
Concerted							
Asp_w→TS1N_w→product	50.62	52.24	3.02×10^{-26}	15.19	2.77	14.95	9.30×10^{-3}
Step-wise							
Asp_w→TS2Nb_w→product	55.74	56.38	2.77×10^{-29}				
Cyclic Intermediate							
Asp_w→TS3Nc_w→product	53.76	55.77	7.77×10^{-29}				
Assisted systems							
Concerted							
Asp_w2→TS1N_w2→product	41.95	43.84	4.37×10^{-20}	20.39	−1.45	20.82	1.16×10^{1}
Step-wise							
Asp_w2→TS2Nb_w2→product	41.25	43.07	1.60×10^{-19}				
Cyclic Intermediate							
Asp_w2→TS3Nc_w2→product	56.98	59.71	1.00×10^{-31}				

[a] Rate constant computed based on Eq. 1

Acknowledgments This research work was supported financially by The Thailand Research Fund, co-funded by The Commission of Higher Education and The Faculty of Engineering, Rajamangala University of Technology Isan, Khonkaen campus through the young academic research grant no. MRG5380243 to W.S., which is gratefully acknowledged.

References

1. Pan B, Ricci MS, Trout BL (2006) Biochemistry 45:15430–15443
2. Chu JW, Yin J, Brooks BR, Wang DIC, Ricci MS, Brems DN, Trout BLJ (2004) Pharm Sci 93:3096–3102
3. Liu DTY (1992) Trends Biotechnol 10:364–369
4. Kosky AA, Razzaq UO, Treuheit MJ, Brems DN (1999) Protein Sci 8:2519–2523
5. Wei W (1999) Int J Pharm 185:129–188
6. Krug JP, Popelier PLA, Bader RFW (1992) J Phys Chem 96:7604–7616
7. Antonczak S, Ruizlopez MF, Rivail JL (1994) J Am Chem Soc 116:3912–3921
8. Bakowies D, Kollman PA (1999) J Am Chem Soc 121:5712–5726
9. Kahne D, Still WC (1988) J Am Chem Soc 110:7529–7534
10. Brown RS, Bennet AJ, Slebockatilk H (1992) Acc Chem Res 25:481–488
11. Bryant RAR, Hansen DE (1996) J Am Chem Soc 118:498–5499
12. Radzicka A, Wolfenden R (1996) J Am Chem Soc 118:6105–6109
13. Gorb L, Asensio A, Tunon I, Ruiz-Lopez MF (2005) Chem Eur J 11:6743–6753
14. Cascella M, Raugei S, Carloni P (2004) J Phys Chem B 108:369–375
15. Zahn D (2004) Eur J Org Chem 19:4020–4023
16. Pan B, Ricci MS, Trout BL (2011) J Phys Chem B 115:5958–5970
17. Pan B, Ricci MS, Trout BL (2010) J Phys Chem B 114:4389–4399
18. Wang B, Cao Z (2010) J Phys Chem A 114:12918–12927
19. Catak S, Monard G, Aviyente V, Ruiz-Lopez MR (2008) J Phys Chem A 112:8752–8761
20. Catak S, Monard G, Aviyente V, Ruiz-Lopez MR (2006) J Phys Chem A 110:8354–8365

21. Joshi AB, Kirch LE (2004) Int J Pharm 273:213–219
22. Joshi AB, Rus E, Kirch LE (2000) Int J Pharm 203:115–125
23. Joshi AB, Sawai M, Kearny WR, Kirch LE (2005) J Pharm Sci 94: 1912–1927
24. Herrman KA, Wysocski VH (2005) J Am Soc Mass Spectrom 16: 1067–1080
25. Oliyai C, Borchardt RT (1993) Pharm Res 10:95–102
26. Stewart JJP (1989) J Comput Chem 10:221–264
27. Parr RG, Young W (1989) Density functional theory of atoms and molecules. Oxford University Press, Oxford
28. Hohenberg P, Kohn W (1964) Phys Rev B 136:864–871
29. Khon W, Sham L (1965) J Phys Rev A 140:1133–1138
30. Beck AD (1993) J Chem Phys 98:5648–5652
31. Lee C, Yang W, Parr R (1988) Phys Rev B 37:785–789
32. Madura J, Jorgensen WL (1986) J Am Chem Soc 108:2517–2527
33. Tomasi J, Mennucci B, Cancés E (1999) J Mol Struct (THEOCHEM) 464:211–226
34. Cancès ET, Mennucci B, Tomasi J (1997) J Chem Phys 107:3032–3041
35. Mennucci B, Tomasi J (1997) J Chem Phys 106:5151–5158
36. Mennucci B, Cancès ET, Tomasi J (1997) J Phys Chem B 101: 10506–10517
37. Cossi M, Barone V (1998) J Chem Phys 109:6246–6254
38. Barone V, Cossi M, Tomasi J (1997) J Chem Phys 107:3210–3221
39. Cossi M, Scalmani G, Rega N, Barone V (2002) J Chem Phys 117: 43–54
40. Frisch MJ et al (2003) Gaussian 03. Revision B.03. Gaussian, Pittsburgh
41. Flükiger P, Lüthi HP, Portmann S, Weber J (2000) MOLEKEL 4.3. Swiss Center for Scientific Computing, Manno
42. Ochterski JW (2000) Thermochemistry in Gaussian. Gaussian, Pittsburgh
43. Ruangpornvisuti V (2009) Int J Quant Chem 109:275–284
44. Bravo-Perez G, Alvarez-Idaboy JR, Cruz-Torres A, Ruiz ME (2002) Phys Chem A 106:4645–4650
45. Wigner EZ (1932) Phys Chem B 19:203–216
46. Hirschfelder JO, Wigner E (1939) J Chem Phys 7:616–628
47. Bell RP (1980) The tunnel effect in chemistry. Chapman and Hall, London
48. Zhao Y, Truhlar DG (2008) Theor Chem Acc 120:215–241
49. Sang-aroon W, Ruangpornvisuti V (2013) J Mol Model 19(9):3627–3636
50. DaCosta H, Fan M (2012) Rate constant calculation for thermal reactions: methods and applications. Wiley, Hoboken, NJ
51. Zhang S, Basile FJ (2007) Proteome Res 6:1700–1704
52. Loudon GM (1983) Organic chemistry. Addison-Wesley, Reading, MA
53. Geiger T, Clarke S (1987) J Biol Chem 262:785–794
54. Voorter CE, de Haard-Hoekman WA, van den Oetelaar PJ, Bloemendal H, de Jong WW (1988) J Biol Chem 263:19020–19023